Benchmarking of debris flow experimental tests using combined finite-discrete element method, FEMDEM

Benchmarking of debris flow experimental tests using combined finite-discrete element method, FEMDEM

F. Vagnon[1], A.M. Ferrero[1], J.P. Latham[2], and J. Xiang[2]

[1]Department of Earth Science, University of Turin, Turin, Italy
[2]Department of Earth Science and Engineering, Imperial College of London, UK

Numerical simulations of debris flow events provide a useful tool for investigating, within realistic geological contexts, the dynamics of these phenomena. One application of such numerical models is to evaluate and forecast impact loading on protection barriers. Most of these models are uncoupled methods: this means that it is necessary to use different codes for analysing the motion phase and for evaluating impact forces. In this way, the uncertainties related to the barrier design are increased and difficult to quantify. In this paper the combined finite-discrete element method, FEMDEM is employed to back-analyse experimental impact tests of debris flow interacting against rigid and waterproof barrier. This methodology allows the simultaneous determination of flow characteristics (velocity and thickness) and impact load on the barrier structure. Two different numerical set-ups were adopted to reproduce laboratory experiments. In the first case, we defined *a priori* the size and the shape of the impacting particles. In the second case, the unstable mass was hypothesised as a unique block with fracture joint elements behaviour, cohesionless, and very low tensile strength. In this way the gravity and friction forces led the particles flowing into the flume. The results were compared in order to quantify the effects of the set-up schemes and material characteristics on the simulations. Limitations and future developments on the application of FEMDEM methodology to this type of geotechnical problem are discussed.

INTRODUCTION

Forecasting debris flow motion characteristics and impact loads on obstacles is an essential component of landslide risk assessment, but it is still a big challenge. The runout prediction provides a mean of defining the susceptible areas, estimating the debris flows intensity and working out the information for the individuation and design of appropriate protective measures (Pirulli and Sorbino, 2008). Concerning the evaluation of debris flow motion characteristics, numerical simulations can provide a useful tool. In the attempt of modelling landslide dynamics, many methods based on continuum (Savage and Hutter, 1989; Hungr, 1995; Pirulli, 2005; Pastor *et al.,* 2009) or discontinuum (Will and Konietzky, 1998; Richefeu *et al.,* 2012) mechanics have been developed. The outputs of these models are fundamental for the design of countermeasures and they are used as inputs in codes (*e.g* Brighenti, Segalini, and Ferrero, 2013; Hungr and Kellerhals, 1984) for evaluating impact forces on structures.

This procedure, based on uncoupled models, presents some limitations: (i) the evaluation of motion characteristics does not take into account the construction of countermeasures; (ii) the impact pressure is calculated considering maximum values of flow characteristics, neglecting time dependence of the phenomenon; (iii) in risk assessment, the evaluation of residual risk after barrier construction is particularly arduous.

With increasing computing power and the development of discontinuous deformation analysis (Shi and Goodman, 1989), it is clear that purely continuum or purely discontinuum models become inadequate to simulate landslide phenomena (Stead, Eberhardt, and Coggan, 2006).

Hybrid finite-discrete element methods (FEMDEMs) overcome the previous stated limitations and allow the contemporary analysis of initiation, propagation, and impact phase in landslide-protection structure systems.

Concerning debris flow processes, this method introduces an innovative approach, since it is possible to evaluate simultaneously motion characteristics and induced stresses on the barrier.

In order to highlight advantages and limitations in the application of this methodology for the design of debris flow protection structures, small-scale debris flow experimental tests were numerically simulated, and the results are here discussed.

FEMDEM NUMERICAL METHOD

In the 1990s, Munjiza and co-workers (Munjiza, Owen, and Bicanic, 1995; Munjiza and White, 1999) developed a comprehensive combined finite-discrete element method (FEMDEM). This two-dimensional code was named Y2D code and is available on VGeST (Virtual Geoscience Simulation Tools).

The FEMDEM model combines the finite strain elasticity with a smeared crack model and is able to capture the behaviour of discontinuum systems involving deformation, rotation, interaction, fracturing, and fragmentation (Latham *et al.*, 2017). The code introduces internal fracturing properties for each particles: this means that if stresses are sufficient to propagate cracks and initiate failure in the particles, they will fragment and the DEM formulations will continue to track the fragment motions. It schematizes the combined fracture-matrix solid system of a 2D fractured rock (Figure 1a) using three-noded triangular finite elements and four-noded joint elements embedded between edges of triangular elements (Figure 1b). The joint elements can be divided into cohesive (unbroken) joint elements and fracture (broken) joint elements. The deformation of the bulk material is captured by the linear-elastic constant-strain triangular finite elements with the impenetrability enforced by a penalty function and the continuity constrained by a constitutive relation for cohesive joint elements (Munjiza and White, 1999), while the interaction of matrix bodies through discontinuity interfaces is simulated by the penetration calculation (Munjiza and Andrews, 2000) along fracture joint elements. An algorithm based on the original continuous configuration between triangular elements in the matrix domain allows the construction of cohesive joint elements. The formation of fracture joint elements is based on the initial configuration of overlapping edges of the opposite triangular elements along pre-existing fractures. The joint elements (either broken or unbroken) are created and embedded between the edges of triangular element pairs before the numerical simulation, and no further re-meshing process is performed during later computations.

Both classic Coulomb type friction law (Xiang, Munjiza, and Latham, 2009) and joint constitutive model based on Barton-Bandis work (Lei, 2016) are implemented in the code, introducing innovative insights in FEMDEM approach.

The equations are solved by an explicit time integration scheme based on the forward Euler method. In Y2D code there are three parameters that play a fundamental role in the simulations: the viscous damping coefficient μ, the penalty number p, and the computation time step.

The viscous damping coefficient is an artificial parameter to counteract energy imbalance during contact between particles. It is given by the following equation:

$$\mu \leq \frac{1}{2} h \sqrt{E\rho} \qquad [1]$$

where h is the minimum element edge, E is the Young's Modulus and ρ the density of the material.

The penalty number is introduced with the aim of eliminating the drawbacks of the Lagrange multipliers method to enforce contact constraints and of imposing an impenetrability condition. The physical meaning of penalty number comes through the concept of a contact layer, which is in a way crude approximation of surface roughness. The relation used for its determination is:

$$p = 2 \sim 100 \cdot \frac{E\nu}{(1+\nu)(1-2\nu)} \quad [2]$$

where ν is the Poisson's ratio.

Then, time step evaluation is related to penalty number concepts and both to the minimum element edge dimension and the minimum element volume. The smaller the mesh dimension, the smaller the time step required. The minimum time step can be evaluated as:

$$t = \min\left(\frac{h}{10\sqrt{\frac{E}{\rho}}}; \frac{1}{10\sqrt{\frac{\rho A}{p}}}\right) \quad [3]$$

where A is the minimum element volume.

For further details on this method, the reader can refer to Munjiza (2004), Munjiza, Knight, and Rougier (2011), and Guo, Latham, and Xiang, (2015).

In brief, FEMDEM approach has the capability to simulate the whole process of rock slope failure from fracture initiation and propagation to deposition. Furthermore, taking advantage of FEM principles, this methodology is ideal for the simulation of interaction between rock particles and protection structures.

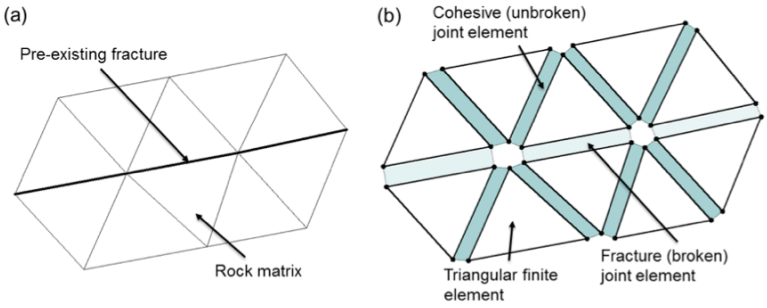

Figure 1. Representation of (a) a 2D fracture-matrix solid system using a mesh consisting of (b) three-noded triangular elements and four-noded cohesive/fracture joint elements embedded between edges of triangular elements (Lei, 2016).

BENCHMARKING OF DEBRIS FLOW EXPERIMENTAL TESTS

Experimental Set-up and Procedure

The previously described methodology was used for simulating debris flow laboratory tests performed in a steel flume 4 m long, 0.39 m wide, and 0.7 m tall in which a rigid barrier was positioned orthogonally at the channel bottom. The slope was 35°. The flow was started by the sudden emptying of a hopper into the flume (Figure 2). Motion characteristics (velocity and flow thickness) were measured using four ultrasonic level measurers, mounted along the centre line of the channel; the normal thrust acting on the barrier was acquired using four load cells installed at the plate vertices.

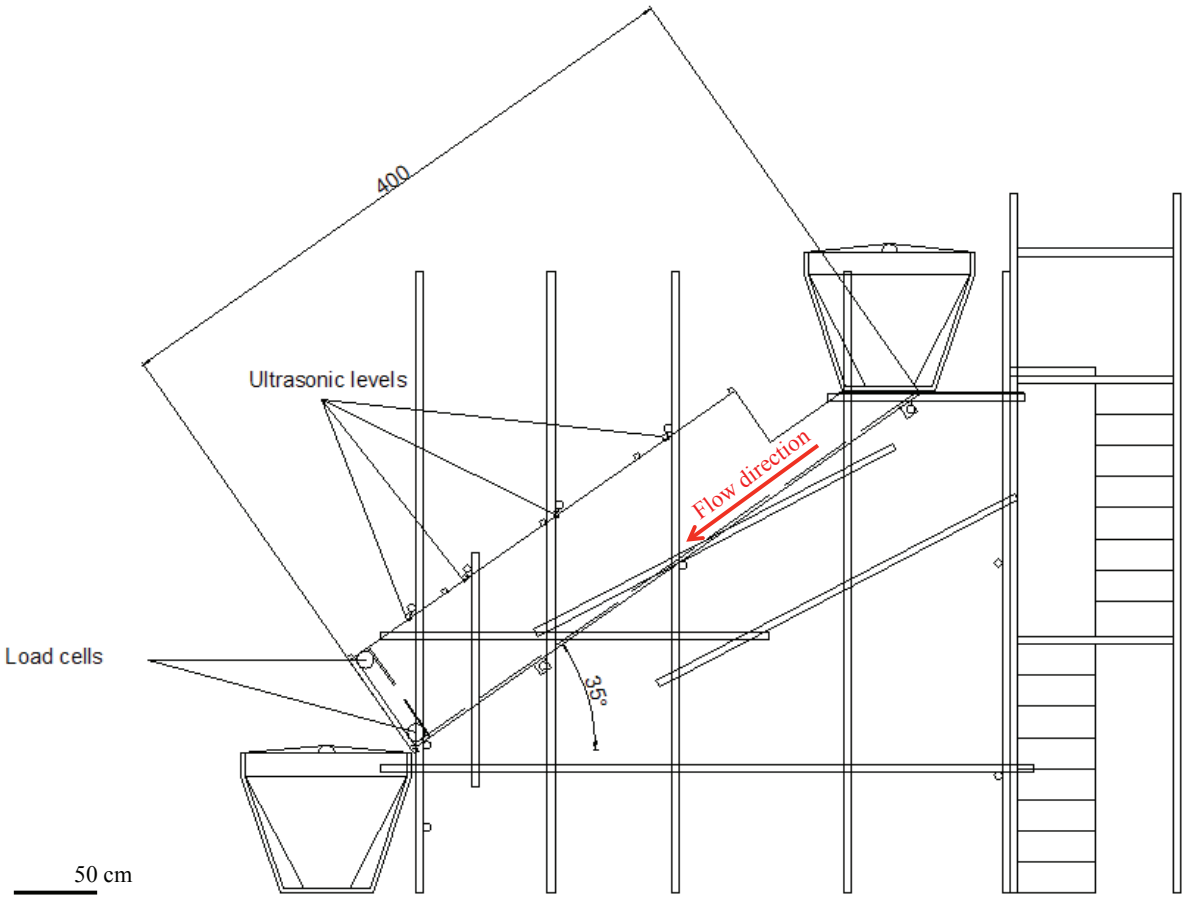

Figure 2. Schematic of the flume and of the starting mechanism.

Tests were performed using sand in order to consider a homogeneous fluid scheme for evaluating the peak thrust and to avoid the formation of overpressures due to the impact of boulders and their interactions inside the flow. The sand volume released into the flume was equal to 0.0624 m^3. The flume section is 0.39 m wide in the third dimension (not show in Figure 2) and is of rectangular form.
The performed tests are characterized by two main phases: the hopper filling by the sand particles and the particle release into the flume.

More details about experimental set-up and execution procedure are available in Vagnon and Segalini (2016).

Experimental Test Simulations
One feature of the FEMDEM code that is different from the common numerical continuum models, in which it is very complicated to accurately reproduce the experimental procedure, is the ability to simulate the material filling and releasing phase.

Concerning the set-up of numerical simulations, two different approaches were used. The first approach (NA1) consists of schematizing the laboratory mixture using three different particle shapes (triangular, square, and heptagonal) with maximum dimension equal to 0.01 m. In the second approach (NA2), the unstable mass is considered as a unique intact block that quickly disaggregates, by modelling fracture behaviour with joint elements and a Mohr-Coulomb criterion with no cohesion and hypothesising a very low angle of internal friction (friction coefficient equals to 0.6); and also later for the contact between particles, the friction coefficient is the same value (friction coefficient equals to 0.6), as implied by the angle of repose of the sand in the experiments.

For the NA1 approach, the numerical simulation can be divided into two phases: the first one is the hopper filling and the second one is the release of material into the flume. In the NA2 approach, only the releasing phase is simulated; this approach is the common one adopted in other numerical models (continuum or discontinuum). The results of the two approaches are here discussed and compared with the experimental values.

Since Y2D is a two-dimensional code, the first issue was the evaluation of the areal distribution of the unstable mass. In order to obtain this input parameter, the mixture volume was divided by the flume width (0.39 m). Starting from the areal distribution of the mass, the number of particles used in NA1 was defined as a function of the particle surface (cf. Table I).

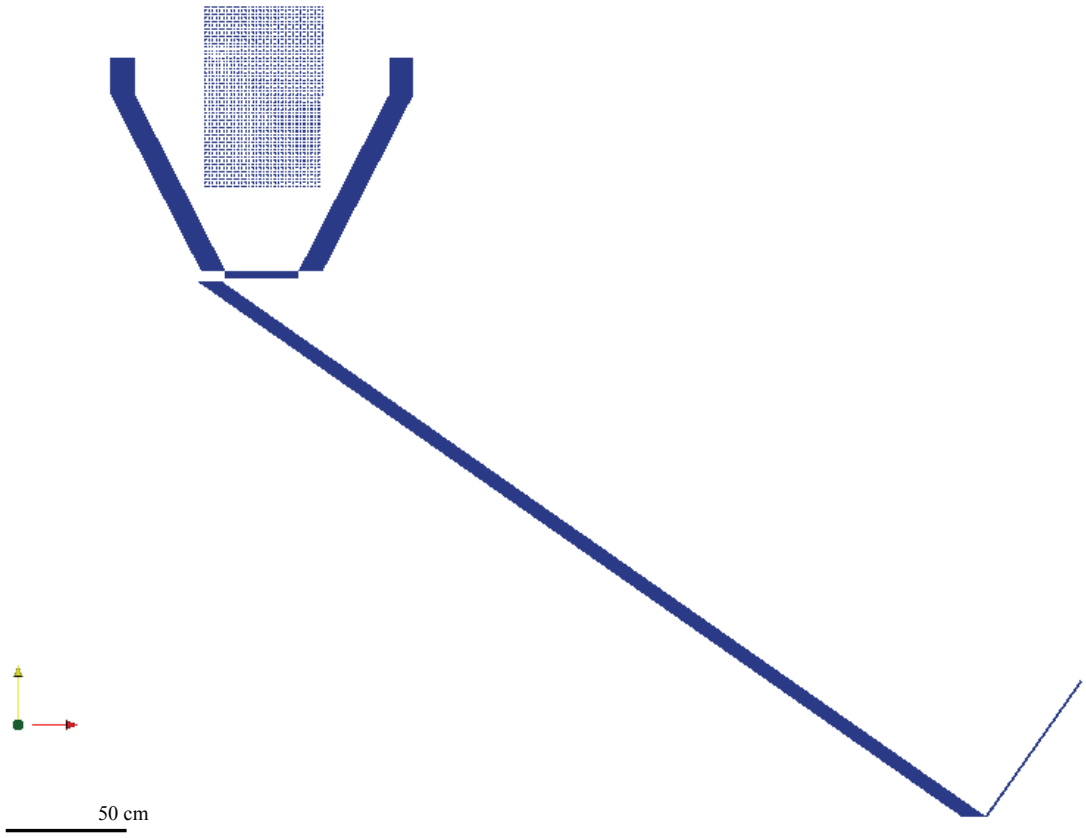

Figure 3. Numerical set-up for simulation approach NA1. Note, hopper base plate can be moved to the right for release.

Figure 3 shows the NA1 simulation set-up: as previously stated, in these simulations both the hopper and flume accurately reproduced those used in laboratory experiments. Material properties assigned to the hopper, the flume, and the rock particles and problem data are listed in Table I. Sand characteristics used in numerical simulation were selected based on experimental test characteristics. Damping coefficient, penalty number, and dimension of time steps were assigned using the equations presented in the previous section. In particular the time step was evaluated using Equation [3]: it was observed that if the time step was insufficiently small (*e.g.* greater than values reported in the column 'time step' of Table I), either the simulation crashed or the results presented numerical instability.

Table I. Material characteristics and problem data for Y2D simulations using NA1.

Numbers of particles							
Triangular shape					4022		
Square shape					1600		
Heptagonal shape					1600		
Material characteristics							
Material	Assigned to…	Young's modulus [Pa]	Poisson's ratio	Friction coefficient	Tensile strength [Pa]	Internal friction coefficient	Cohesion constant [Pa]
Sand	Particles	1,00E+10	0,3	0,95	1,00E+06	0,5	0
Steel	Hopper, flume and barrier	2,11E+11	0,3	0,2	3,60E+08	0,95	8,00E+06
Problem data							
Problem name	Particle shape	Material	Penalty number choosen [Pa]	Damping coefficient [kg/(m*s)]	Time step [s]		
hoptr	triangular	sand	1E+11	1,71E+04	1,29E-08		
		steel	1E+12	1,36E+05			
hopsq	square	sand	1E+11	1,71E+04	5,11E-08		
		steel	1E+12	1,36E+05			
hopept	heptagonal	sand	1E+11	1,71E+04	2,77E-08		
		steel	1E+12	1,36E+05			

For the mesh dimension, triangular elements with edge length of 0.01 m were drawn both for particles and for the rigid barrier. Both particles and experimental set-up were modelled assigning 2D solid elastic behaviour. No-displacement boundary conditions were imposed at each node of the hopper and flume (each mesh point had velocity equal to zero). Concerning the barrier, only basal points (those in contact with the flume surface) were held fixed.

In order to reproduce the hopper filling and the natural random particle packing, the digital particles were created numerically in the pre-processor to be arranged following a regular grid and were located a certain distance from the bottom of the hopper (Figure 3); during the first phase of numerical simulation, the hopper filling was driven by the gravity. By assigning a horizontal velocity to the base plate of the hopper, the fast opening of the hopper and the consequent releasing of particles were simulated.

Triangular and square shapes showed some problems, especially during the releasing phase (Figure 4). Due to their high angularity, the simulations performed using these shapes resulted in the formation of arching effects in the hopper, or in the case of squares, the vertical stacking and blocking up of the base of the flume prevented the particle flowing into the channel. For these reasons, numerical results of these simulations are not reported and analysed in this paper.

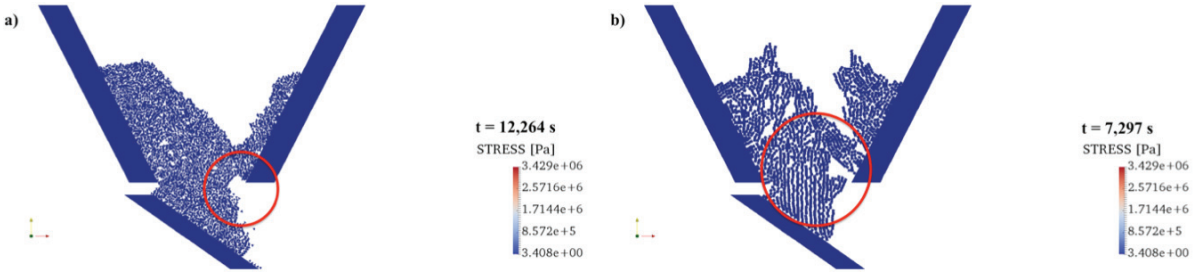

Figure 4. Particular of the releasing phase in numerical simulations using triangular particles (a) and square particles (b). Red circles highlight the formation of arch effects and vertical piling due to the particle shape.

Particles with heptagonal (seven-sided) shape better described the performed experimental tests. In contrast to the other cases (triangular and square shape) the complete emptying of the hopper was observed. Moreover, heptagonal shape showed a better capability to reproduce experimental tests in terms of propagation velocity (see Figure 5 and Table III). Also in terms of stress induced by the impact into the barrier, numerical results carried out using this particle shape fitted the experimental data better (Figure 6).

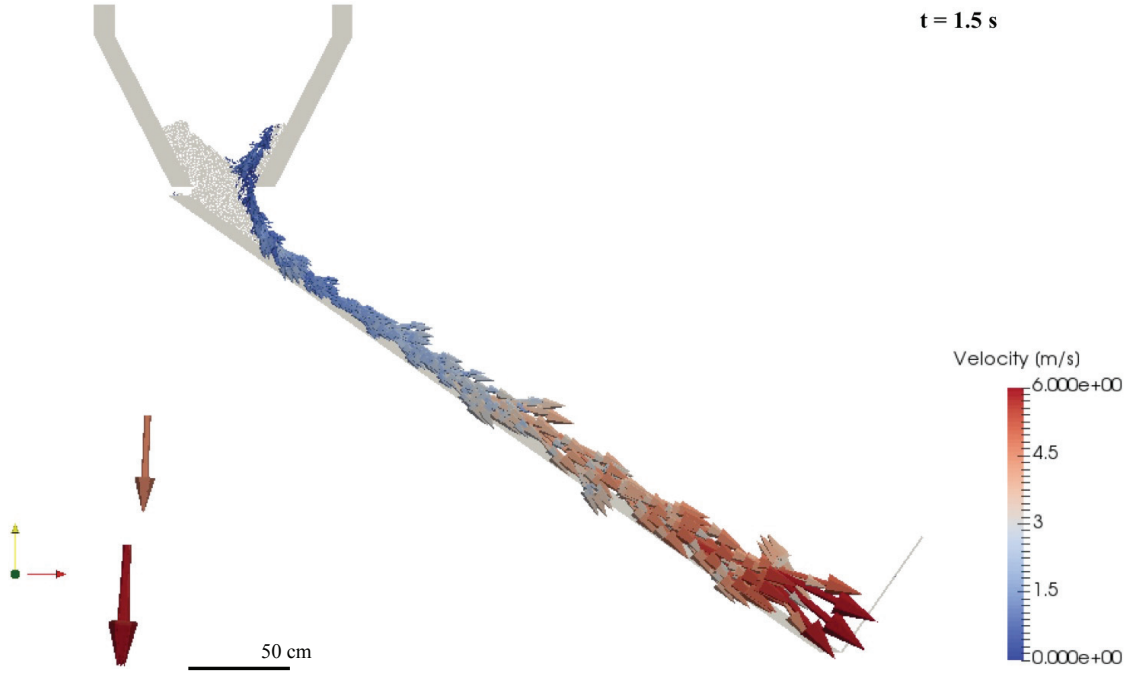

Figure 5. Particle releasing into the flume and correspondent velocity values.

Since the load cells were located at the barrier vertices, the total horizontal force acting on the middle point of the barrier was evaluated as the sum of those recorded at each sensor. In order to compare the experimentally measured force with the internal numerical stress trend acting on the point at the base of the barrier element, a scheme of a cantilever beam with fixed support was adopted. In this way, the experimental stress induced inside the barrier was calculated as the sum of two components: one induced by the barrier weight and the other generated by the momentum induced by the measured total impact thrust. Numerical and experimental stress results are reported in Figure 6.

During the flow impact, the basal points of the barrier are the most stressed: this aspect is particularly important for designing debris flow protection structures. Thus, in this paper we wanted to show the

capability of the FEMDEM code to reproduce the trend of the induced stress in the barrier due to the impact of particles, in terms of both maximum and residual values. The numerical fluctuation of the results is a consequence of the barrier oscillation. In fact, points at the base of the barrier are in a state of traction that increases as consequence of the particle impact but, due to the elastic behaviour of the barrier, it can decrease (blue line in Figure 6). This fluctuation was not observed in experimental data since the sensors were capable of recording only compressive forces.

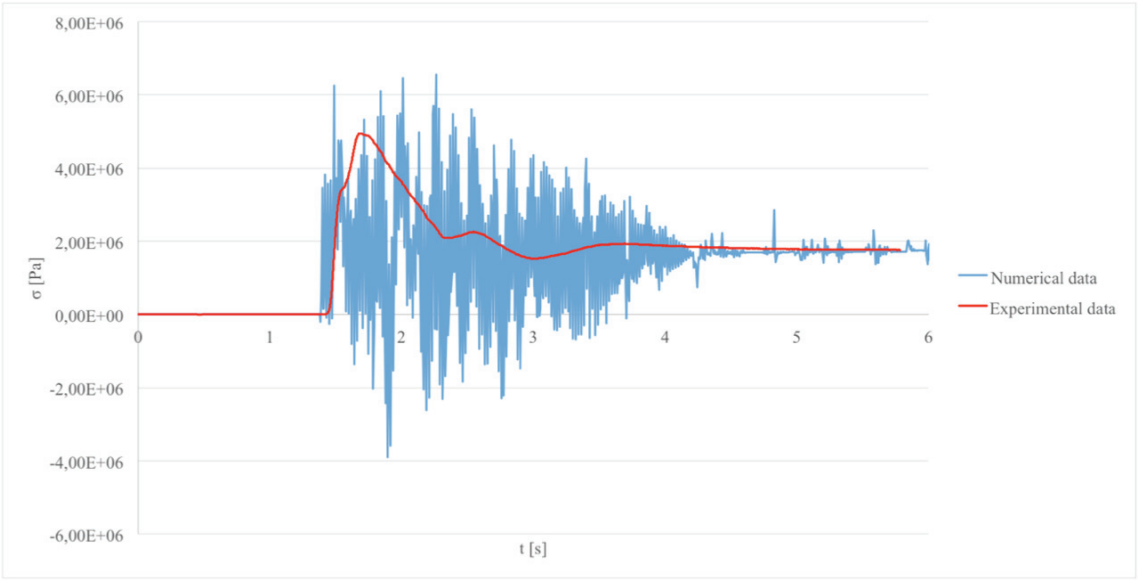

Figure 6. Comparison between numerical stress (blue line) and experimental stress (red line) trend at the bottom of the barrier for NA1 simulation using particles with heptagonal shape.

In simulation NA2, instead of representing the flow generated by a certain number of particles, the same conceptual strategy adopted for the continuum numerical approach was used. In this case, the hopper was not represented and the flume length was increased to 6 m (Figure 7). This approach consisted of representing the initiation phase in a different way with respect to described experimental tests. This procedure is common in continuum numerical simulation in which it is very complicated to faithfully reproduce the real triggering mechanism. Thus, we checked that the numerical velocity values in correspondence of the first ultrasonic level were the same as in the experimental test. Under this hypothesis we increase the flume dimension of 2 m.

Furthermore, the unstable mass was idealized as an intact block that would rapidly disaggregate in accordance with fracture joint element behaviour informed by cohesion-less and very low tensile strength intact properties (Table II). Due to the gravity and friction forces, the particles started to flow down into the flume.

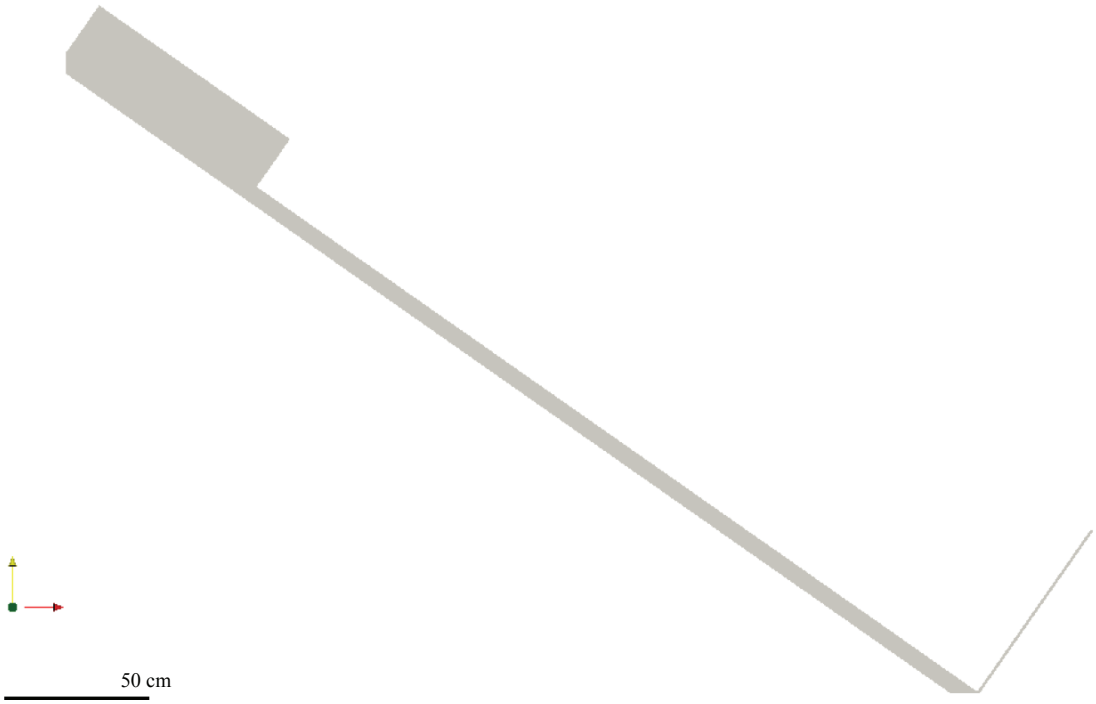

Figure 7. Numerical set-up for simulation approach NA2.

Table II. Material characteristics and problem data for Y2D simulations using NA2.

Material characteristics							
Material	Assigned to…	Young's modulus [Pa]	Poisson's ratio	Friction coefficient	Tensile strength [Pa]	Internal friction coefficient	Cohesion constant [Pa]
Sand	Unstable Mass	1,00E+10	0,3	0,6	1,00E+00	0,6	0
Steel	Hopper, flume and barrier	2,11E+11	0,3	0,2	3,60E+08	0,95	8,00E+06
Problem data							
Problem name	Particle shape	Material	Penalty number choosen [Pa]	Damping coefficient [kg/(m*s)]	Time step [s]		
fract	triangular	sand steel	1,00E+08 1E+12	6,34E+02 1,36E+05	4,1E-08		

The simulations were analysed following the same procedure used for NA1. Figure 8 and Figure 9 present the trend of the numerical and experimental stress evaluated at the bottom of the rigid barrier and the distribution of particle velocity before impact. The computed velocity values are lower than those obtained in NA1 simulations (Figure 9 and Table III). This could be related to the relative ease with which heptagons roll compared with the triangular shape of the typical disaggregated pieces making up the flow in NA2. This explains the lower stress values, especially considering the dynamic

phase (that is governed by impact) compared with the static one (that is governed by the build-up of particle deposition behind the barrier). About the fluctuation of the results, the same considerations made for the case of NA1 are valid, *i.e.* the flexing of the barrier.

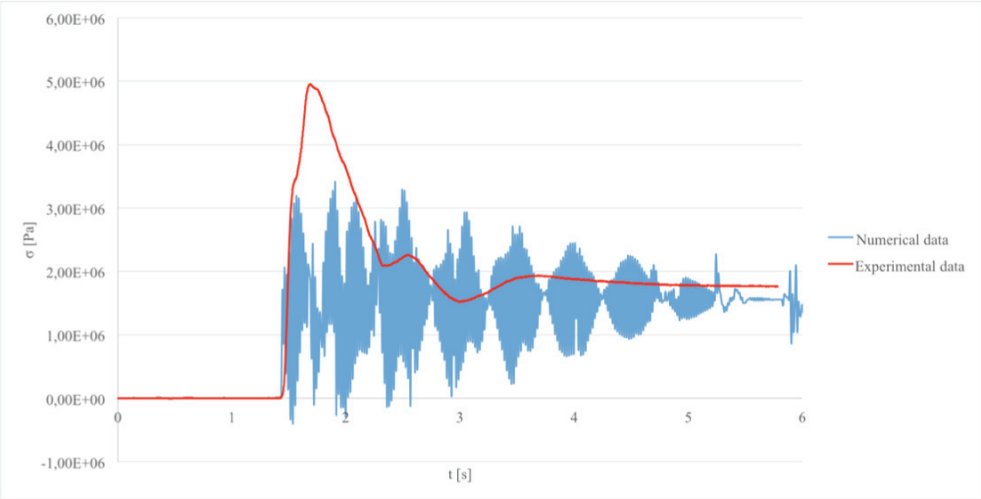

Figure 8. Comparison between numerical stress (blue line) and experimental stress (red line) trend at the bottom of the barrier for NA2 simulation.

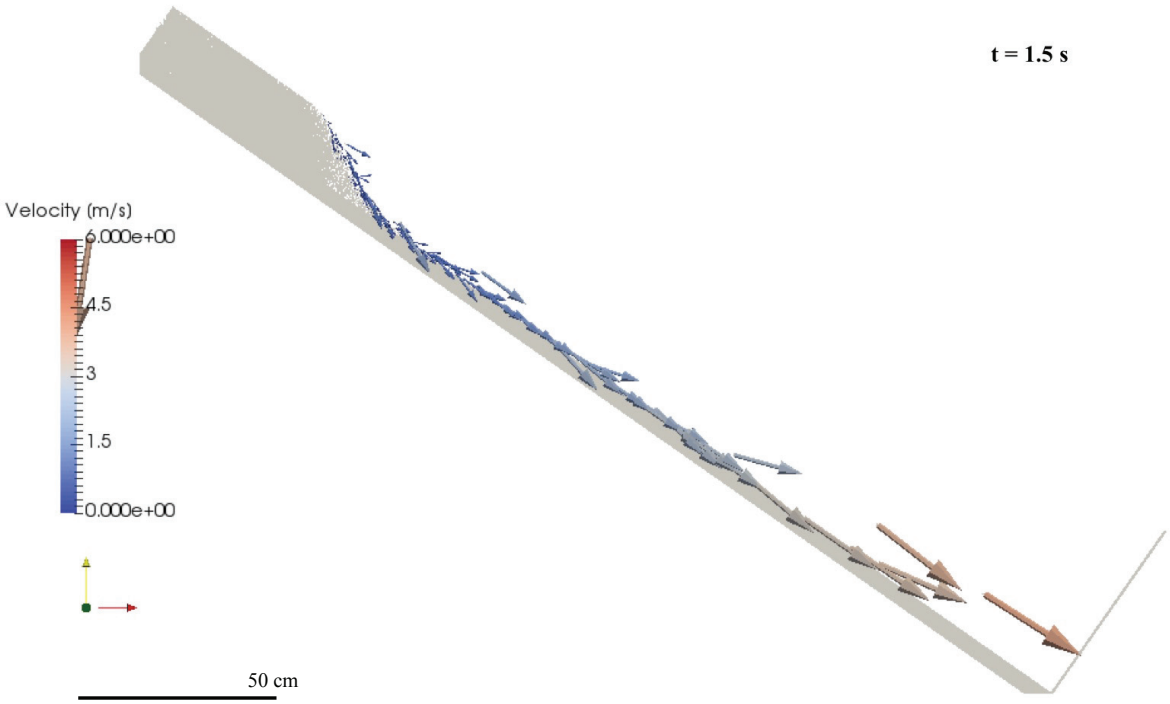

Figure 9. Distribution of particle velocity values evaluated in NA2. Note, the disaggregating, initially rectangular, pile of material

Table III. Comparison between numerical and experimental results.

	NA1	NA2	Experimental tests
Velocity at the impact [m/s]	6	4,5	5,96±0,84
Maximum stress at the bottom of the barrier [MPa]	6,56	3,4	4,95±0,94

DISCUSSION, AND CONCLUSIONS

The FEMDEM simulation tool provides numerous opportunities to study fundamental mechanisms in rock slide avalanches. In particular it is very useful for evaluating the interaction between the sliding body and protection structures.

In this paper, a first attempt at simulating debris flow propagation and interaction with a structure using a FEMDEM approach is presented, paying particular attention to key points and possible limitations of this methodology.

Small-scale debris flow experiments have been simulated following two different numerical approaches. These numerical approaches required an accurate calibration of both the material (Young's modulus, cohesion, friction coefficient, and tensile strength) and numerical (damping coefficient, penalty number and time step) parameters. Concerning damping coefficient a clarification is required: this damping is due contact only (Munjiza, 2004). Thus, the energy balance and the momentum balance are preserved irrespective of the penalty value, size of penetration, or geometry of the contact because kinetic energy is continuously transformed in potential energy before particle contact and *vice-versa* after contact release.

The results from NA1 showed a good approximation of the experimental test values both in terms of impact velocity and maximum stress at the bottom of the barrier. On the other hand, NA2, which follows a more classical way to numerically schematize debris flow experimental tests, tends to underestimate laboratory values, probably due to the rolling resistance of excessively angular discrete particles in the simulation (see Table III).

Regarding the stress comparison with experiments, the resulting dynamic fluctuations shown in Figure 6 and 8 are the consequence of the total elastic behaviour of the barrier: in fact, the impact energy of the blocks produces a temporary and reversible displacement that stops after the block is seen in the simulation to bounce. In this way, the points at the bottom of the barrier constantly swing between a state of traction and compression. The fluctuation reaches a constant value, which corresponds to the static pressure, during the filling of the barrier. Once more, this fact demonstrates the hypothesis for considering the impact force as the sum of a dynamic component and a static one (Vagnon and Segalini, 2016), both essential for design considerations.

The previously described results highlight the excellent potentialities of the FEMDEM methodology in the reproduction of landslide behaviour. In particular, it allows the simulation of the interaction between landslides and protection structures, considering simultaneously the effects of flow propagation. However, it still has some limitations due to the lengthy computational time required to perform simulations with fine mesh. This limitation depends on both computer calculation power and minimum mesh dimension. Since in these types of models, the mesh dimension is fundamental and it

has to be fine for reproducing the real particle dimension, the simulations last a very long time (several days).

Considering these two numerical approaches, further analysis should be made to try to reduce the effect of particle shape: for instance, it will be useful to create random particles, inducing cracking into an intact rock (Xiang *et al*., 2010) with weak characteristics and comparing the real grain size distribution with the reproduced one. Finally, the use of a 3D FEMDEM approach would furnish further insights for the analysis of debris flow phenomena.

REFERENCES

Brighenti, R., Segalini, A., and Ferrero, A.M. 2013. Debris flow hazard mitigation: A simplified analytical model for the design of flexible barriers. *Computers and Geotechnics*, 54, 1–15.

Guo, L., Latham, J.P., and Xiang, J. (2015). Numerical simulation of breakages of concrete armour units using a three-dimensional fracture model in the context of the combined finite-discrete element method. *Computer and Structures*, 146, 117-142.

Hungr, O. (1995). A model for the runout analysis of rapid landslides, debris flows and avalanches. *Canadian Geotechnical Journal*, 32 (4), 610-623.

Hungr, O., Morgan, G.C., and Kellerhals, R. (1984). Quantitative analysis of debris torrent hazards for design of remedial measures. *Canadian Geotechnical Journal*, 21(4), 663-677.

Latham, J.P., Xiang, J., Obeysekara, A., Lei, Q., Yang, P., Salinas, P., Pavlidis, D., and Pain, C. (2017). Modelling hydro-geomechanical behaviour of fractured and fracturing rock masses: application to tunnel excavation-induced damage. *Proceedings of MIR 2017, Innovazioni nella Progettazione, Realizzazione, Gestione delle Opere in Sotterraneo*, Torino. Celid, Torino. pp. 79-95.

Lei, Q. (2016). Characterisation and modelling of natural fracture networks: geometry, geomechanics and fluid flow. PhD thesis, Imperial College, London.

Munjiza, A., Owen, D.R.J., and Bicanic, N. (1995). A combined finite-discrete element method in transient dynamics of fracturing solids. *Engineering with Computers*, 12, 145-174.

Munjiza, A. and White, J.K. (1999). Combined single and smeared crack model in combined finite-discrete element analysis. *International Journal for Numerical Methods in Engineering*, 44 (1), 41-57.

Munjiza, A. and Andrews, K.F.R. (2000). Penalty function method for combined finite-discrete element systems comprising large number of separate bodies. *International Journal for Numerical Methods in Engineering,* 49, 1377-1369.

Munjiza, A. (2004). *The Combined Finite-Discrete Element Method*. Wiley, Chichester, UK.

Munjiza, A., Knight, E.E., and Rougier, E. (2011). *Computational Mechanics of Discontinua*. Wiley, Chichester, UK.

Pastor, M., Haddad, B., Sorbino, G., Cuomo, S., and Drempetic, V. (2009). A depth integrated coupled SPH model for flow-like landslides and related phenomena. *International Journal for Numerical Methods in Geomechanics*, 33 (2), 143-172.

Pirulli, M. (2005). Numerical modelling of landslide runout, a continuum mechanics approach. PhD thesis, Department of Structural and Geotechnical Engineering, Politecnico di Torino, Italy.

Pirulli, M. and Sorbino, G. (2008). Assessing potential debris flow runout: a comparison of two simulation models. *Natural Hazards and Earth System Sciences*, 8, 961-971.

Richefeu, V., Mollon, G., Daudon, D., and Villard, P. (2012). Dissipative contact and realistic block shapes for modelling rock avalanches. *Engineering Geology*, 149-150, 78-92.

Savage, S.B. and Hutter, K. (1989). The motion of a finite mass of granular material down a rough incline. *Journal of Fluid Mechanics*, 199, 177-215.

Shi, G.H. and Goodman, R.E. (1989). Generalization of two-dimensional discontinuous deformation analysis for forward modelling. *International Journal for Numerical and Analytical Methods in Geomechanics*, 13 (4), 359-380.

Stead, D., Eberhardt, E., and Coggan, J.S. (2006). Developments in the characterization of complex rock slope deformation and failure using numerical modelling techniques. *Engineering Geology*, 83 (1-3), 217-235.

Vagnon, F. and Segalini, A. (2016). Debris flow impact estimation on a rigid barrier. *Natural Hazards Earth System Science*, 16, 1691-1697. doi:10.5194/nhess-16-1691-2016.

Will, J. and Konietzky, H. (1998). Neue techniken der numwrike zur berechnung von felsboschungen. *Felsbau*, 16, 155-167.

Xiang, J., Munjiza, A., and Latham, J.P. (2009). Finite strain, finite rotation, quadratic tetrahedral element for the combined finite-discrete element method. *International Journal for Numerical and Analytical Methods in Geomechanics*, 79, 946-976.

Xiang, J., Latham, J.P., Harrison, J., and Zhang, Z.Q. (2010). A numeric simulation of rock avalanches using the combined finite-discrete element method, FEMDEM. *Proceedings of 44th US Rock Mechanics Symposium and 5th US-Canada Rock Mechanics Symposium (ARMA)*, Salt lake City, Utah. American Rock Mechanics Association, Alexandra, VA

Dr. Federico Vagnon

Researcher
Turin University

Dr. Federico Vagnon (fvagnon@unito.it) is a researcher in Geotechnics and Applied Geology at the Earth Sciences department of the Turin University since January 2014. He obtained his PhD in February 2017 with the thesis entitled "Theoretical and experimental study on the barrier optimization against debris flow risk". His research topics are related to: i) the definition of debris flow impact pressure on structures; ii) the numerical simulation of rapid landslides for evaluating both motion characteristics and effects on countermeasures; iii) reliability based methods for defining probability of failure of structures exposed to debris flow phenomena.